Supplementary Material

Source data and R code can be downloaded as a .zip file here:

https://www.dropbox.com/s/mxjpic5votp128k/usl_R_data.zip?dl=0

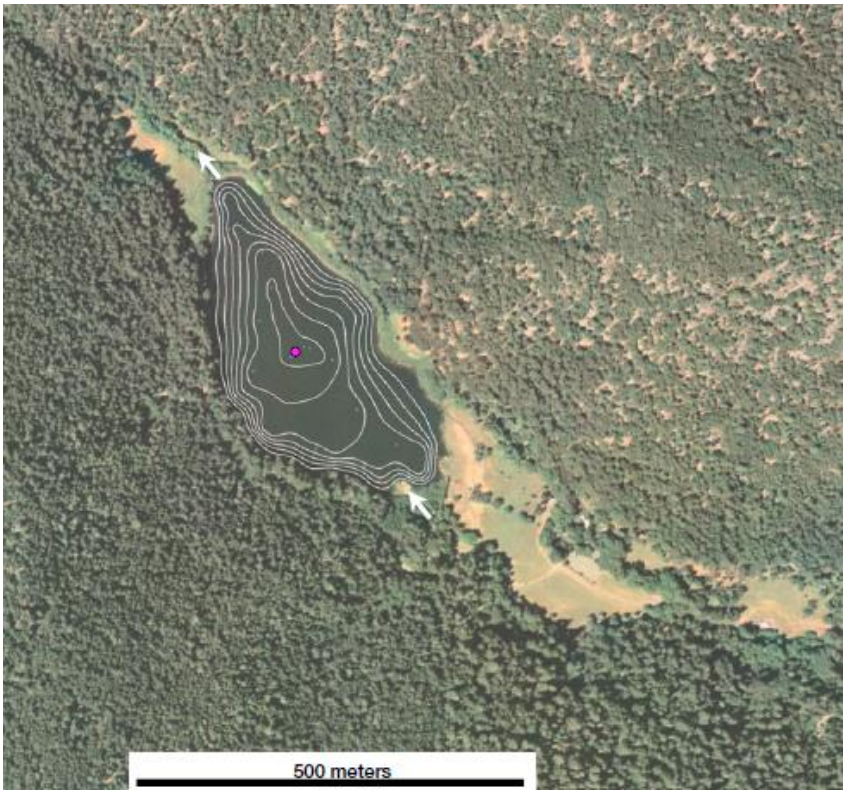

Fig. S1. Bathymetric map of Upper Squaw Lake showing the relatively flat bottom of the lake relative to the coring spot. Arrows indicate inlet/outlet (from Colombaroli and Gavin, 2010).

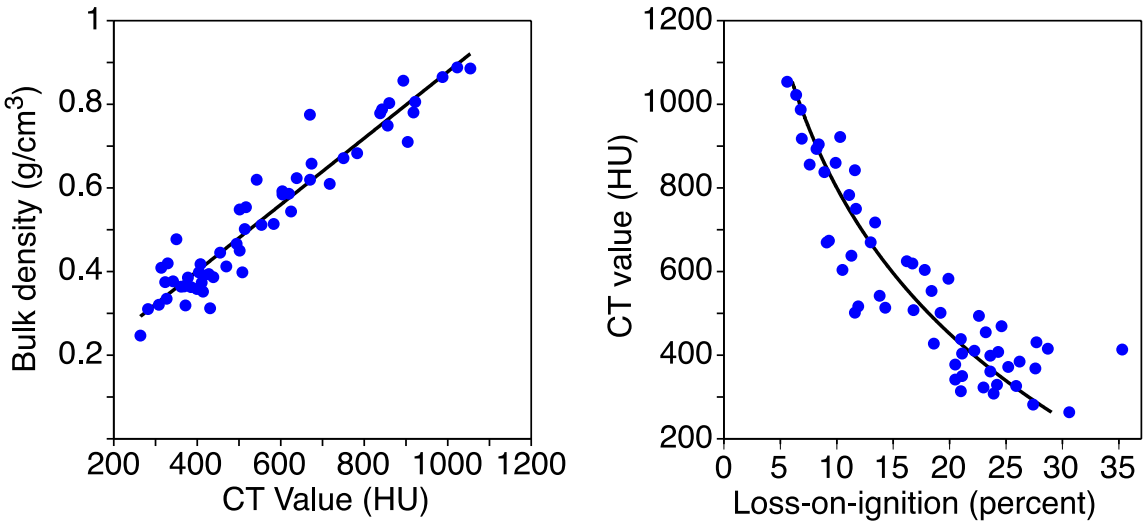

Fig. S2. Radiodensity varies linearly with bulk density and percent organic matter. Bulk density and loss-on-ignition at 550°C were calculated on 1 cm^3 subsamples (reported in Colombaroli and Gavin 2010).

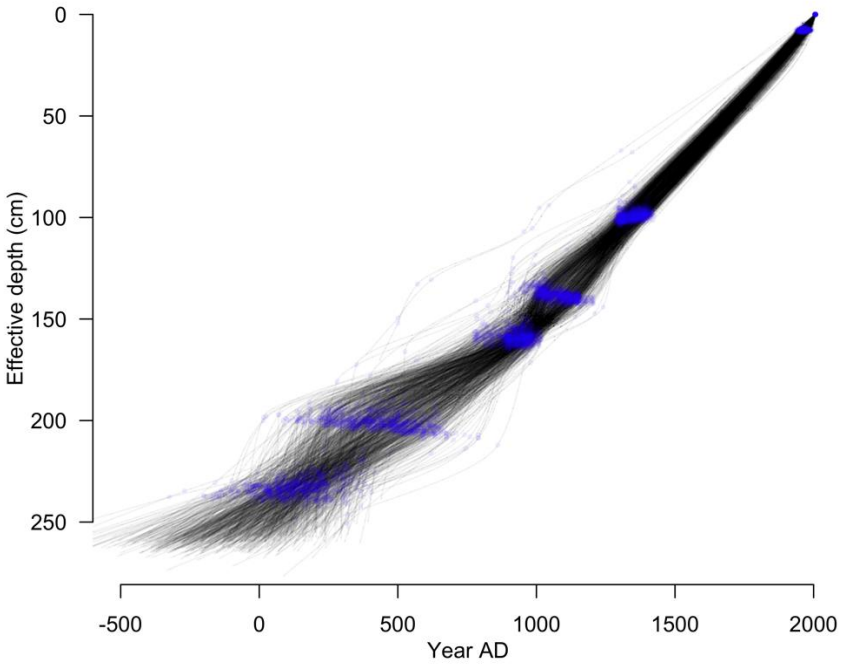

Fig. S3. 1000 simulations the age-depth model from Upper Squaw Lake. Each model is calculated from selecting sample ages from the probability distributions from six radiometric dates (blue dots). For each model, the instantly deposited silt component is estimated from each sample and subtracted from the measured

depth, resulting in the estimated effective depth. A monotonic spline curve is then fit through the samples.

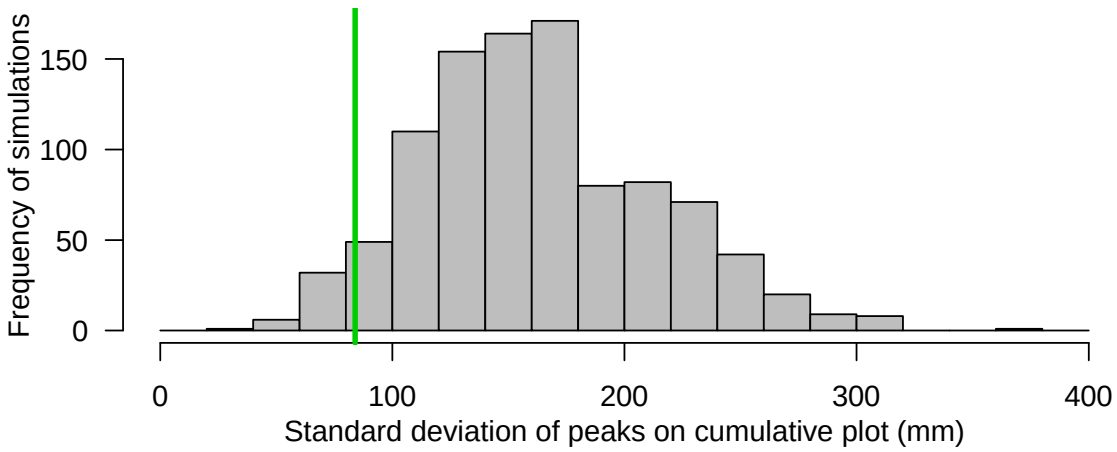

Fig. S4. Standard deviation statistic of accumulated silt values following the seven largest events (blue circles in main text Fig. 5). The observed deviation (green line) is significantly smaller than that expected from randomizing the dates of the events, indicating dependency of event magnitude on time since previous large events.

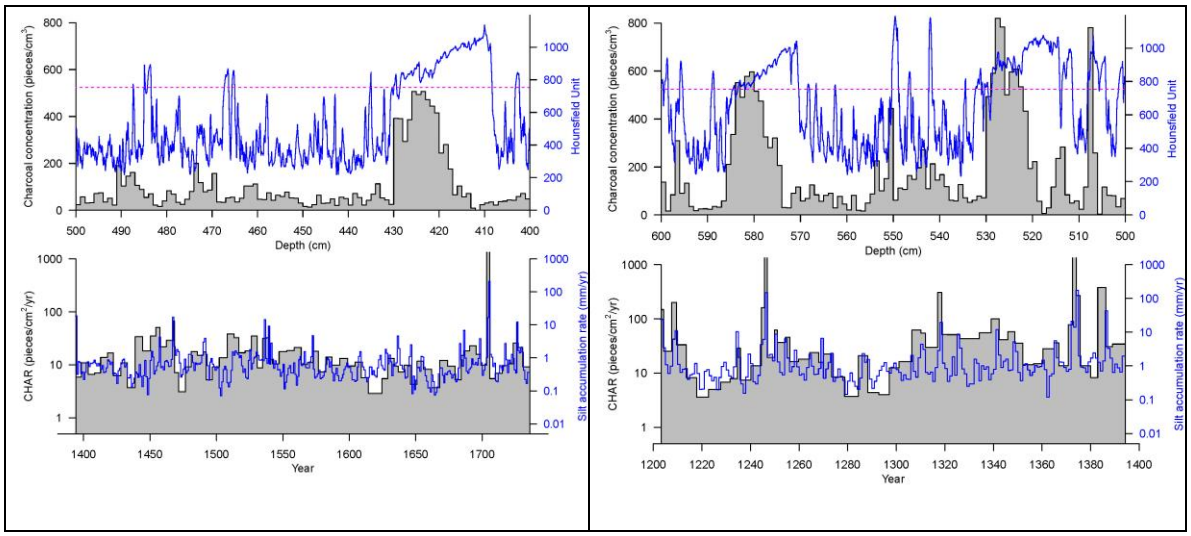

Fig. S5. Charcoal concentration and radiodensity plotted for 1-m long core segments from Upper Squaw Lake (2 selected sections). Charcoal particles were quantified at 1-cm intervals. The lower figure in each plot shows the same core segment plotted on an age scale, in which silt events (marked by high radiodensity) were collapsed into instantaneous events.

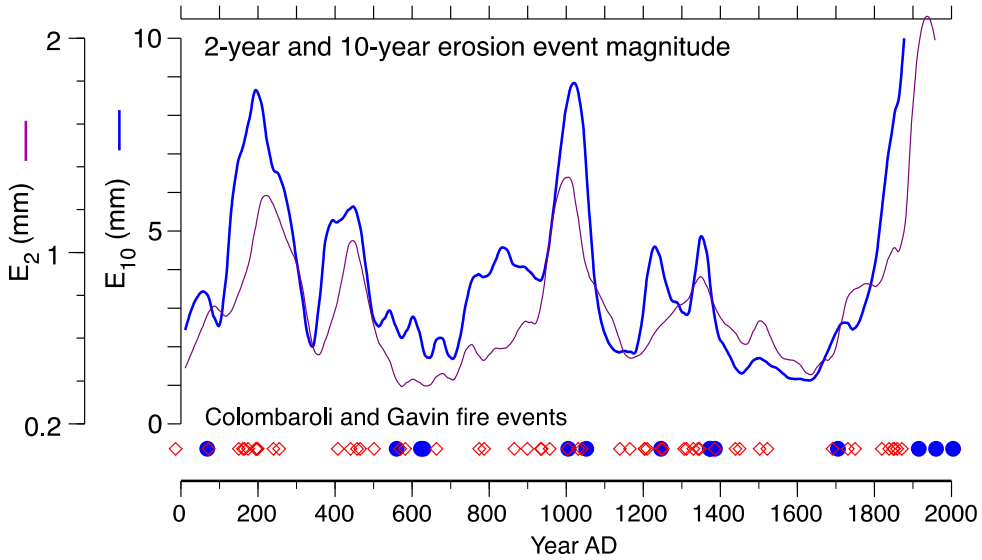

Fig. S6. Comparison of the E2 and E10 erosion magnitude reconstructions with fire dates identified from peaks in the charcoal record (Colombaroli and Gavin 2010). The fire dates were modified from the previous study using the

chronology in the current study. Solid blue circles are the largest charcoal peaks and red diamonds are smaller magnitude events.

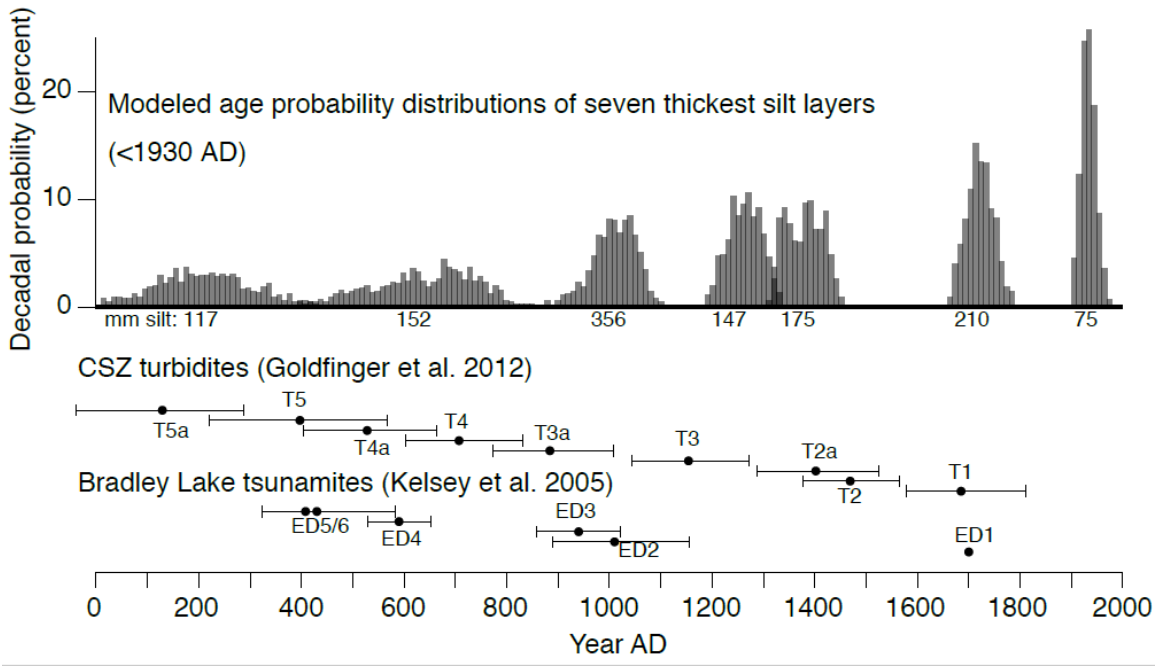

Fig. S7. The age-probability distributions for the seven largest silt events compared to reconstructed M9 Cascadia subduction zone earthquakes as detected from Cascadia Subduction Zone off-shore turbidites (Goldfinger et al., 2012) and a tsunami record from Bradley Lake (Kelsey et al., 2005).